ACS APPLIED MATERIALS & INTERFACES

www.acsami.org

Research Article

Triboelectric Leakage-Field-Induced Electroluminescence Based on ZnS:Cu

Jiayu Li, Zhiwei Zhang, Xiongxin Luo, Laipan Zhu,* and Zhong Lin Wang*

Cite This: *ACS Appl. Mater. Interfaces* 2022, 14, 4775−4782

Read Online

ACCESS | Metrics & More | Article Recommendations | Supporting Information

ABSTRACT: The related studies and applications of ZnS-based phosphorescent materials involve various aspects such as lighting, display, sensing, electronic signatures, and confidential information. Here, triboelectrification-induced electroluminescence (TIEL) of the ZnS:Cu due to the triboelectric leakage field is discovered via a gently horizontal sliding between a ZnS:Cu particle-doped polydimethylsiloxane (PDMS) film and a polytetrafluoroethylene (PTFE) or fluorinated ethylene propylene (FEP) film, whose intensity is positively correlated with the temperature, the doping ratio of ZnS:Cu, the pressure, and the frequency. It is also demonstrated that the TIEL mainly occurs inside the bulk film, where the ZnS:Cu phosphor particles can be polarized instantaneously by the leakage electric field of triboelectrification. The polarization will lead to a tilted energy band of the ZnS, resulting in an emitting of green light due to electrons detrapped into the conduction band and recombined with holes in the impurity state. This study not only reveals great fundamental physics for understanding of luminescence induced by a simple sliding between two triboelectric materials but also indicates another way for triboelectrification to be used in advanced optoelectronic devices.

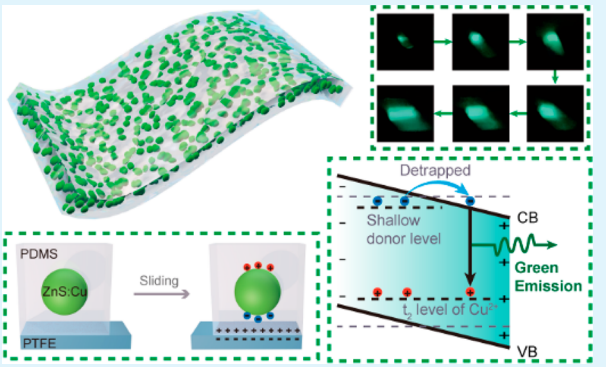

KEYWORDS: *triboelectrification, electroluminescence, ZnS:Cu, phosphor, flexible*

INTRODUCTION

The luminescence of ZnS:Cu was first discovered by a French chemist in 1866.[1] However, it was not until 1936 that the first study of Cu-doped ZnS was published and green luminescence was observed.[2] Since then, studies on the alternating current (AC) electroluminescence (EL) of ZnS:Cu have been gradually carried out.[3−5] By studying the mechanism as well as the properties of EL of ZnS:Cu in the following decades, it is generally regarded as a typical phosphorescent material capable of generating blue and green emissions. Among them, the green light emission is considered to result from the following processes: electrons are excited from the valence band to the conduction band, which are subsequently trapped by the shallow donor level below conduction band and further recombined with holes on the impurity state of Cu.[6−8] Researchers have also doped ZnS:Cu phosphor powder into polymer substrate to carry out studies related to AC thin film electroluminescence (AC-TFEL).[9] The ZnS:Cu thin film is able to excite light emission through mechanical stress,[10−13] an electric field,[13−15] photo absorption,[16−18] and a magnetic field.[19] There are a wide range of applications, including lighting,[20,21] display,[15,22−24] sensing,[25−27] electronic signatures,[28] and confidential information.[29] In addition, there are diverse opinions about its EL mechanism. In recent years, someone proposed that the EL of ZnS:Cu thin films is derived from a type of triboelectrification-induced electroluminescence (TIEL), which relies on a coupling of triboelectrification and EL.[30−33] However, current studies related to TIEL have several limitations. First, for horizontal sliding derived luminescence using a sharp object on a triboelectric material, a large pressure is usually generated because of the extremely small contact area, so that both TIEL and mechanoluminescence (ML) are present, and the magnitude of their contributions is difficult to distinguish. Second, although the surface of the phosphorescent composite film can emit light, it is inconclusive whether the ZnS:Cu phosphor particles inside it are participating in luminescence. Third, it is also unknown whether the luminescence process is related to the high-voltage discharge caused by air breakdown. Thus, it would be intriguing to design TIEL devices that can be implemented by slight horizontal sliding, as it can not only help people understand the mechanism of TIEL in depth but also avoid the abrasion of the sample surface by sliding under higher pressure, so as to improve the lifetime of the device.

Received: November 30, 2021
Accepted: January 5, 2022
Published: January 12, 2022

In this work, a polydimethylsiloxane (PDMS)/ZnS:Cu composite was fabricated to investigate the EL mechanism of ZnS:Cu thin films. A separate object affixed with the triboelectric material films underneath, for instance, polytetrafluoroethylene (PTFE), fluorinated ethylene propylene (FEP), polyvinyl chloride (PVC), polyethylene glycol terephthalate (PET), polyethylene (PE), Nylon, Kapton, Cu. and Al, was prepared to horizontally slide against the PDMS/ZnS:Cu composite film, and a green light emission from the PDMS/ZnS:Cu composite along the motion trajectory of the slider can be observed. Because of the presence of a leakage electric field inside the PDMS/ZnS:Cu composite film resulting from an uneven friction between the two triboelectric materials, the energy band of the ZnS at both the surface and the bulk of the film is tilted, which helps the electrons trapped in the shallow donor level escape to the conduction band and then recombine luminescence with the holes on the Cu impurity state. The proposed EL mechanism derived from the leakage electric field is original, which not only provides a deep insight into the fundamental physics of TIEL but also opens up another mode for triboelectrification used in optoelectronic devices.

RESULTS AND DISCUSSION

The ZnS:Cu phosphor powder was uniformly mixed into a colloidal solution with a mass ratio of PDMS and curing agent of 10:1, and then spin-coated on a 4 cm × 1.5 cm transparent acrylic sheet. After curing, the PDMS/ZnS:Cu composite film was fabricated with a thickness of about 22 μm (Figure 1a).

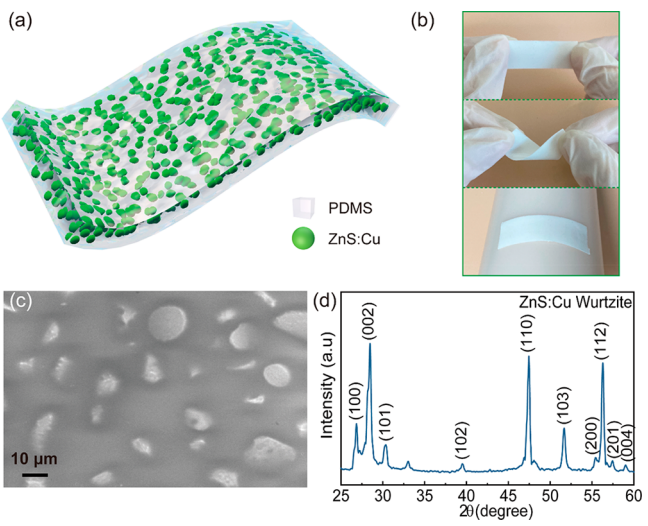

Figure 1. Structure of the PDMS/ZnS:Cu composite. (a−c) Schematic, photographs and ESEM image of the PDMS/ZnS:Cu composite. (d) XRD patterns of the ZnS:Cu phosphor.

Figure 1b shows the optical images of the flexible composite film. The composite film is milky white and translucent and possesses excellent flexibility, which can be bent, twisted, stretched. Through the environmental scanning electron microscope (ESEM) image (Figure 1c), it shows that the ZnS:Cu phosphor powder is dispersed and wrapped in the PDMS matrix. The lattice planes (002), (110), and (112) with 2θ values of 28.500, 47.561, and 56.392° in the X-ray diffraction (XRD) pattern represent the wurtzite structure of ZnS (Figure 1d).

To quantify the TIEL characteristics, we constructed a test setup showed as Figure 2a. A holder with a platform was made by cutting acrylic. The center of the platform contains a circular hole with a diameter of 8 mm, which is designed to embed the optical fiber probe of the spectrometer (approximately 7.7 mm in diameter) just into the hole. The optical fiber probe was fixed immovably with a clamp when the upper slider performed a horizontal sliding reciprocating motion. Subsequently, the composite film fixed with an acrylic substrate was placed directly above the platform, covering the hole where the optical fiber probe was inserted. After that, the triboelectric materials attached to the bottom of the slider rubbed against the PDMS/ZnS:Cu composite in a horizontal sliding motion. Spectra excited from the composite could be captured along the motion trajectory of the slider by the optical fiber probe head on the back. A spectrum was obtained of when the PDMS/ZnS:Cu composite was rubbed horizontally against PTFE (Figure 2b) with a peak at 516 nm in the Commission Internationale de L'Eclairage (CIE) green region (Figure 2c). The EL light-emitting phenomenon in the process of sliding from the leftmost end to the rightmost end is shown in Figure 2d. Because ZnS:Cu exhibits photoluminescent properties, when ZnS:Cu undergoes TIEL, its surrounding ZnS:Cu phosphor particles that are not excited to emit light by friction will absorb green light and emit light. Coupled with the long afterglow phosphor properties of ZnS:Cu, its luminescence can last for a period of time without disappearing immediately. Therefore, a longer luminescence trajectory larger than the slider area can be observed.

The luminescence intensity of the PDMS/ZnS:Cu composite film was measured by controlling the variables according to the above method for different ZnS:Cu doping ratios, stresses, sliding frequencies, temperatures, and triboelectric material. First, the spectra results show that the EL intensity increases with the increment of the ZnS:Cu doping ratio (Figure 3a), which is due to the density of ZnS:Cu phosphor in the composite increases, and more phosphor particles can be excited to luminescence. Second, by augmenting the frequency of horizontal sliding friction reciprocating motion, the luminescence intensity of the composite gradually enhances (Figure 3b). When the frequency applied to the composite is small (1−5.5 Hz), the luminescence intensity grows rapidly, cause the deformation of the composite during the motion can recover itself before deformation caused by the next sliding motion. When the frequency exceeds 7.5 Hz, the luminescence intensity grows slowly, as the deformation has not fully recovered before the next sliding motion, resulting in an accumulation of deformation and thus a larger deformation, which causes a compression between the slider and the PDMS/ZnS:Cu composite, producing ML. Besides, with the increase in the applied force on the slider, the EL intensity of the composite film is increased (Figure 3c). In addition, when the applied force is between 1 and 5 N, the luminescence intensity increases only slightly, whereas when the applied force reaches 7 N or even higher, the luminescence intensity increases significantly. However, when the force becomes higher, the deformation of the composite film gets more violent, the electric field between the two surfaces is more uneven, and the leakage electric field generated becomes larger. Hence, the polarization electric field generated at the top and bottom ends of each ZnS:Cu particles becomes stronger, so that when the ZnS:Cu phosphor is excited, the luminescence gets more intense. On the other hand, as the force increases, the luminescence of the composite may not only originate from TIEL, but also involve ML, and thus the luminescence

https://doi.org/10.1021/acsami.1c23155
ACS Appl. Mater. Interfaces 2022, 14, 4775−4782

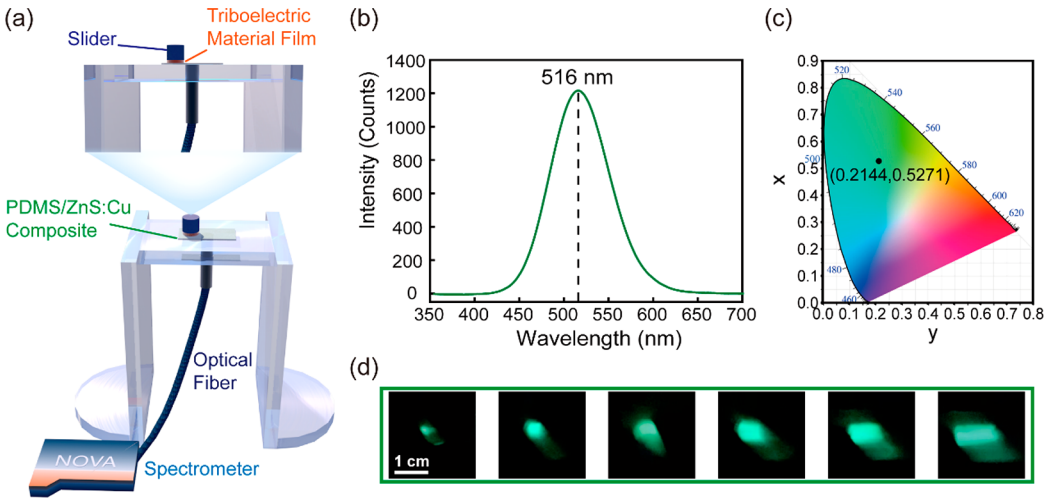

Figure 2. Performance of experimental measurement. (a) Schematic diagram of the test platform for measurement of the TIEL. (b, c) Wavelength spectrum and its CIE coordinates of the PDMS/ZnS:Cu composite. (d) Luminescence induced by a circular slider along a continuous trajectory.

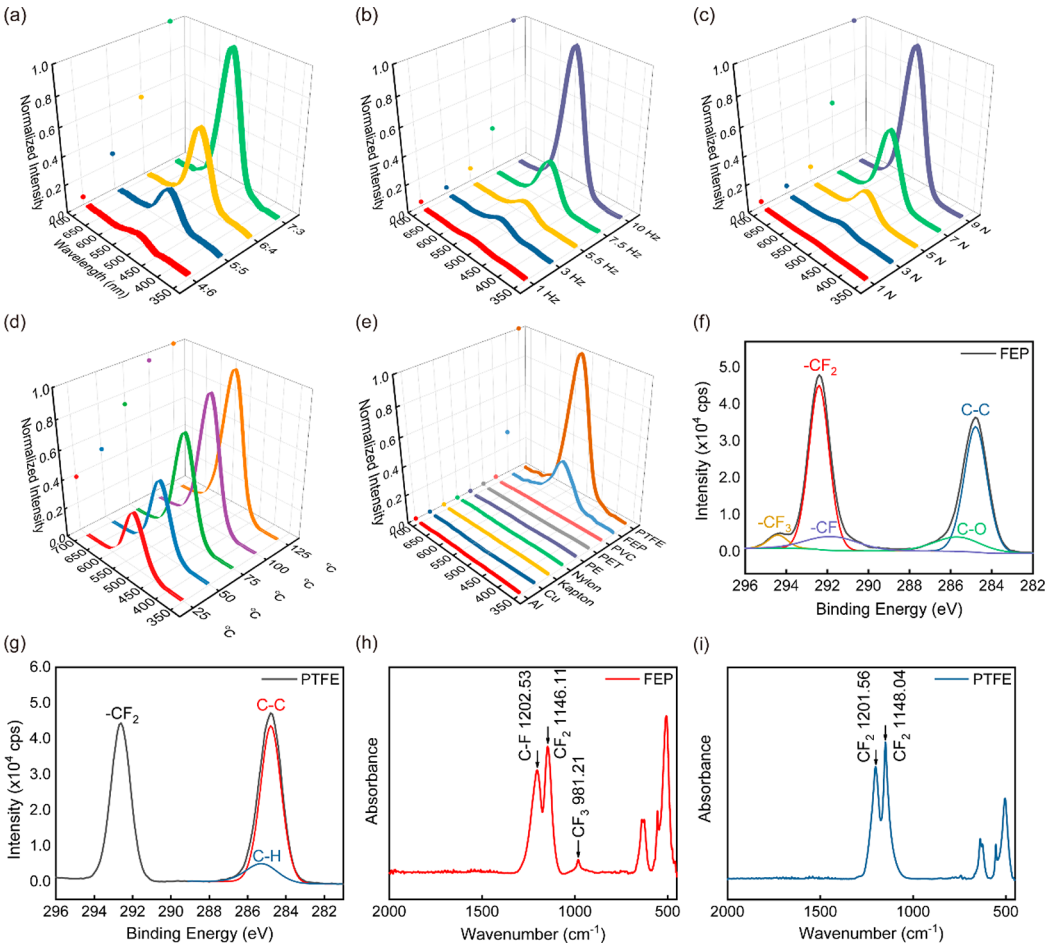

Figure 3. Results of experimental measurement. (a–e) Luminescence intensity of the PDMS/ZnS:Cu composite under different ZnS:Cu phosphor doping ratios, sliding frequencies, stresses, temperatures, and triboelectric materials, respectively. (f, g) XPS images of the (f) FEP and (g) PTFE. (h, i) FTIR images of the (h) FEP and (i) PTFE.

intensity is significantly enhanced under the two luminescence triggering pathways. What's more, when the temperature of the composite film was raised with a heating plate, the spectra were measured at each temperature node. We obtained the effect of temperature on the mechanical properties of PDMS/ZnS:Cu composite conducted by a thermodynamic mechanical analyzer. Figure S1 shows that the elastic modulus of the PDMS/ZnS:Cu composite gradually decreases as the temperature increases from 20 to 130 °C, implying that the film becomes softer, allowing for greater deformation during the sliding process, resulting in a stronger leakage electric field and enhancing the luminescence intensity of the composite (Figure

https://doi.org/10.1021/acsami.1c23155
ACS Appl. Mater. Interfaces 2022, 14, 4775−4782

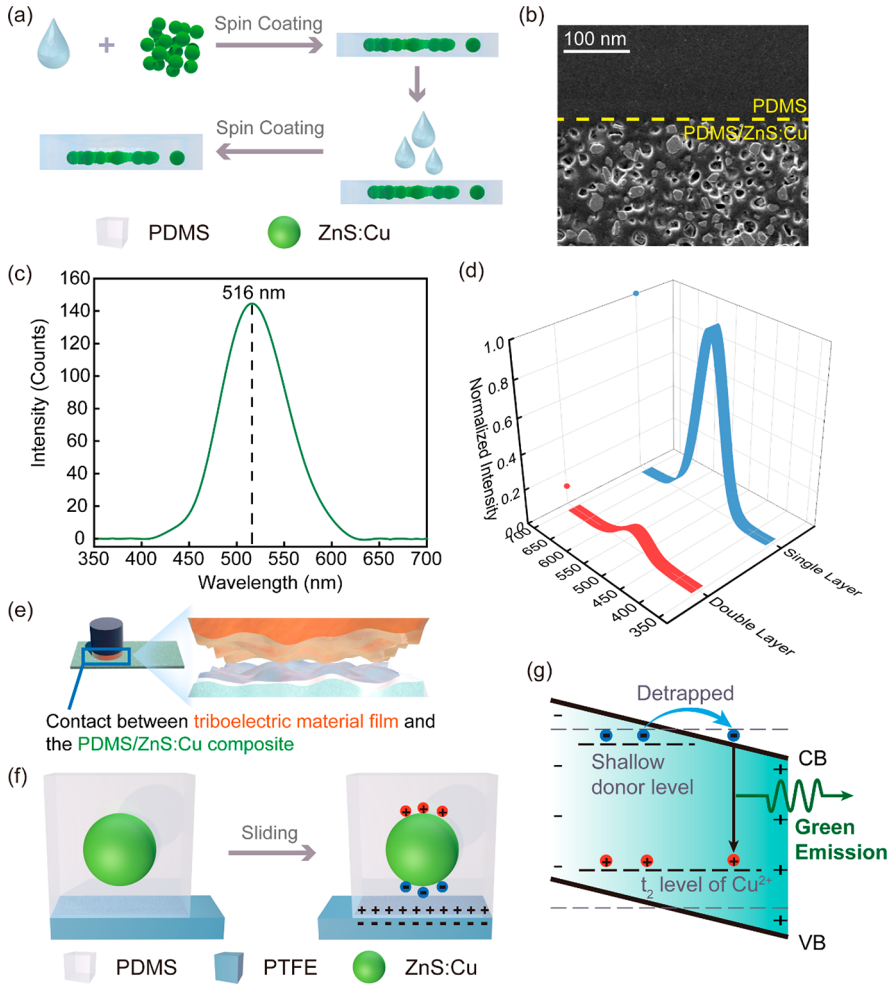

Figure 4. Mechanism analysis of the luminescence of the PDMS/ZnS:Cu composite. (a–c) Schematic of the fabrication process, ESEM image, and wavelength spectra of the PDMS/ZnS:Cu composite with a capping-layer PDMS. (d) Comparison of the light intensity of single-layer and double-layer PDMS of the PDMS/ZnS:Cu composite. (e) Local diagram of the slider in contact with the PDMS/ZnS:Cu composite. (f) Schematic diagram of the charge distribution between the materials. (g) Band diagram describing the TIEL mechanism of the ZnS:Cu phosphor.

3d). In particular, there is a significant reduction in the interval from 20 to 100 °C, and a slight reduction above 100 °C. This trend corresponds to the spectra results, where the luminescence intensity steadily rises between 25 and 100 °C, and with a small increase above 100 °C. Moreover, after rubbing the PDMS/ZnS:Cu composite film with different upper triboelectric materials, it was found that the luminescence occurred only when the composite film was rubbed with PTFE or FEP (Figure 3e). To eliminate the influence of the TENG triboelectric output on luminous intensity, we measured the triboelectric output of the PDMS/ZnS:Cu composite during horizontal sliding reciprocating friction with PTFE, FEP, PET, Cu, PE, Kapton, Nylon, and PVC, respectively (Figure S2). In the sliding friction process, luminescence can be observed only for FEP and PTFE, and the luminescence intensity when rubbed against PTFE is significantly higher than that of FEP. Moreover, in the supplementary TENG output data below, the voltage, current, and charge output of FEP are the highest, reaching 126.3 V, 193.6 nA, and 38.4 nC, whereas the voltage and charge output of PTFE are significantly lower than those of FEP as well as PVC, apparently inconsistent with the trend of luminescence intensity given in the spectra results in Figure 3e. Therefore, we consider that the main factor affecting the luminescence intensity of the PDMS/ZnS:Cu composite is not the triboelectric output of TENG but the leakage electric field intensity. The factors affecting the strength of the leakage field come from two main sources: on the one hand, the enhancement of the leakage field caused by the deformation due to the thermal effect mentioned above, and on the other hand, the electric field intensity between surface of the PDMS/ZnS:Cu composite and the triboelectric materials. Because of the specific surface structure of FEP and PTFE, which can generate more triboelectric charges compared to other triboelectric materials, causing a stronger electric field and leakage electric field between the surfaces of the composite and the triboelectric materials, the leakage electric field has a greater effect on the ZnS:Cu phosphor particles. This concept was further confirmed by the results of the X-ray photoelectron spectroscopy (XPS) and Fourier transform infrared spectrum (FTIR) (Figure 3f-I and Figures S3 and S4). The surface of FEP contains three fluorine-containing chemical bonds $-CF$, $-CF_2$, and $-CF_3$, of which $-CF_2$ is the most abundant (Figure 3f). Additionally, the surface of PTFE merely involves one fluorine-containing chemical bond $-CF_2$ (Figure 3g). Both the surfaces of FEP and PTFE possess a small quantity of C–O or C–H bonds, perhaps on account of the influence of air or residues of substances from the fabrication process. Fur-

https://doi.org/10.1021/acsami.1c23155
ACS Appl. Mater. Interfaces 2022, 14, 4775–4782

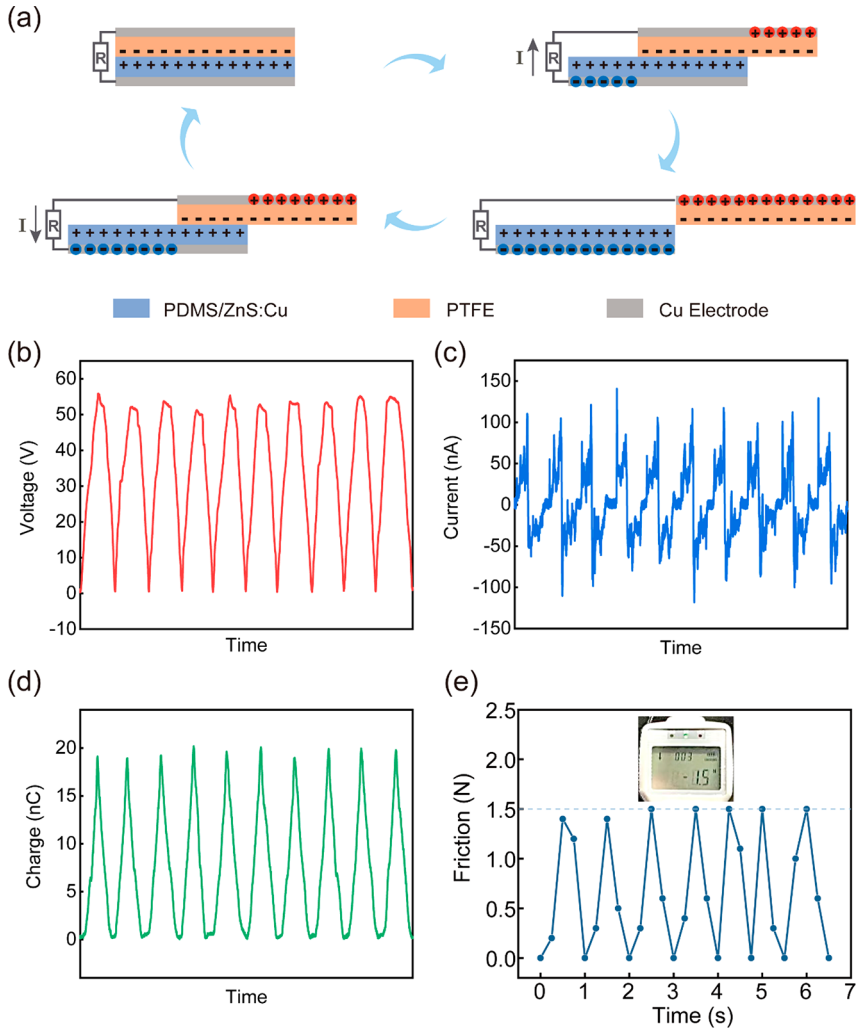

Figure 5. Experimental results excluding the factor of air breakdown. (a) Schematic working principle of the TENG. (b–d) Open-circuit voltage, short-circuit current, and transferred charge amount of the TENG. (e) Frictional force during the TIEL process.

thermore, both of these surfaces have fluorine-containing chemical bonds on the surface, with $-CF_2$ playing a major role. PDMS and other triboelectric materials of PVC, PET, PE, Nylon, Kapton, Cu, and Al have no fluorine-containing chemical bonds on their surfaces. Because the F atom is an electron-absorbing functional group, the C–F bond can greatly heighten the electron-absorbing ability of the polymer, and such ability strengthens with the increase in the number of F atoms linked to C. Accordingly, the C–F bond performs a crucial role in contact triboelectrification. In addition, in the horizontal sliding friction process, PTFE and FEP generate more triboelectric charges thanks to the breakage of fluorine-containing chemical bonds on the surface. On this basis, we used *Comsol* to simulate the electric potential and the electric field between PTFE and the PDMS/ZnS:Cu composite during sliding friction, as well as the effect of the contact condition (Figures S5–S8).

As shown in Figure 4a, the surface of the PDMS/ZnS:Cu composite was spin-coated with another thin layer of PDMS at a thickness of 30 μm to ensure that the ZnS:Cu phosphor powder was completely encapsulated in the PDMS matrix, preventing it from being exposed to the surface. Figure 4b shows a cross-sectional view of the double-layer PDMS/ZnS:Cu composite in an ESEM image. The as-fabricated composite film was subjected to implement a horizontal sliding friction with a PTFE film. Nonetheless, it still triggered a green light-emitting (Figure 4c). However, because of the thickening of the composite, which badly hinders the emission and transmission of the light, the luminescence intensity was weakened when compared with the single-layer composite (Figure 4d). What's more important, it demonstrates that the luminescence of the composite film is emitted from not only the surface but also the inside of the film. In consequence, a new conjecture of the EL mechanism of ZnS:Cu thin films is derived. It can be seen from the horizontal sliding friction sequence that the PDMS surface is positively charged, and correspondingly, the PTFE surface is negatively charged. With regard to those two oppositely charged surfaces in immediate proximity to each other, an electric field will be produced between them. As the PDMS/ZnS:Cu composite film is flexible, a degree of deformation will be consistently generated among the horizontal sliding process (Figure 4e), resulting in a nonuniform electric field between the surfaces. At that time, interaction between inhomogeneous electric fields enormously enhances the leakage electric fields, which act on each of ZnS:Cu phosphor particles inside the composite and induce opposite polarized charges at the upper and lower ends (Figure 4f). Afterward, a local electric field is formed between the

https://doi.org/10.1021/acsami.1c23155
ACS Appl. Mater. Interfaces 2022, 14, 4775–4782

opposite polarized charges, bringing about a bend in the energy band of ZnS, allowing the electrons trapped in the shallow donor level to be lightly detrapped and become free electrons on the conduction band. Finally, the electrons on the conduction band interact with the holes on the deep acceptor level of the impurity state of Cu, occurring with recombination, along with green light emission (Figure 4g).

Furthermore, it is necessary to verify whether air breakdown is a main factor leading to the luminescence of the PDMS/ZnS:Cu composite. A triboelectric nanogenerator (TENG) structure was fabricated by adhering the PDMS/ZnS:Cu composite as well as PTFE to the thin film Cu electrodes respectively (Figure 5a). The principle of TENG lies in the coupling of triboelectrification and electrostatic induction.[34,35] It generates surface electrostatic charges via the contact of two different materials. Meanwhile, the surface charge density increases with the degree of contact between the two dielectrics, eventually reaching saturation. TENG is able to collect mechanical energy and convert it into electrical energy, generating electrical signals. This mechanism can be applied to reflect the surface charge density of the material in the luminescence process of the PDMS/ZnS:Cu composite. Because of the different electron-gaining ability of materials, according to the triboelectric series,[36] triboelectrification results in negative charges on the PTFE surface and positive charges with the same charge density on the surface of the PDMS/ZnS:Cu composite (Figure 5a). The open-circuit voltage, short-circuit current, and transferred charge during the process of horizontal sliding friction reciprocating motion were recorded (Figure 5b–d). The data shows that the amount of charge remained around 20.14 nC. Because of the PDMS/ZnS:Cu composite has a size of 4 cm × 1.5 cm, its area, i.e., the contact area of the TENG is 6 cm^2. The surface charge density of PDMS/ZnS:Cu composite is therefore about 3.36×10^{-4} C m^{-2}. Because of the current and voltage were always kept at about 55.3 V and 117.4 nA, respectively. Without mutational and high signals, coupled with a low surface charge density, it can be concluded that the light-emitting mechanism of the PDMS/ZnS:Cu composite is by no means by air breakdown. In addition, the magnitude of the frictional force for the TIEL process was measured as well (Figure 5e). A dynamometer was attached to the slider to perform horizontal sliding friction. According to the data from the dynamometer, the friction force was always maintained at ~1.5 N, and the area of the slider was about 1.77 cm^2. Thus, the stress of the TIEL was about 8.47 kPa. Nevertheless, the ML normally requires a stress of megapascals, which means the stress in this work is three orders of magnitude smaller than the threshold stress of ML, ruling out the possibility of ML.

CONCLUSIONS

In general, we report a mechanism of triboelectrification-induced electroluminescence that producing a nonuniform electric field between the two surfaces of different materials during the process of horizontal sliding friction, because of the deformation of PDMS/ZnS:Cu composite, which leads to the leakage electric field difficult to ignore and acts on the ZnS:Cu phosphorescent particles inside the composite, causing the energy band of ZnS to be tilted and electrons to be detrapped on the conduction band and finally recombined to emit light on the impurity state of Cu. The luminescence intensity of the PDMS/ZnS:Cu composite increases with the temperature, the frequency, the pressure, and the doping ratio of ZnS:Cu. In addition, a green light emits only when the PDMS/ZnS:Cu composite rubs against FEP or PTFE. Compared with the past studies on TIEL, we emphasize that the luminescence occurs inside the composite except on the surface. In addition, the concept of a leakage electric field that greatly influences the luminescence process during a horizontal sliding friction reciprocal motion was introduced. This study not only reveals great fundamental physics for in-depth understanding of TIEL, but also indicates another way for triboelectrification to be used in advanced optoelectronic devices, especially for application to highly sensitive electronic signature and security monitoring.

EXPERIMENTAL SECTION

Materials. ZnS:Cu (D502CT) was supplied by Shanghai Keyan Phosphor Technology Co., Ltd. Polydimethylsiloxane (Sylgard 184 Silicone Elastomer) with a cross-linker were purchased from Dow Corning. A PTFE thin film was purchased from Chukoh Chemical Industries, Ltd.

Synthesis of PDMS/ZnS:Cu Composite. Dow Corning 184 and curing agent were poured into a beaker at a mass ratio of 10:1, and ZnS:Cu phosphorescent powder was weighed at a mass ratio of 7:3 (ZnS:Cu/Dow Corning 184). Stirred the mixture thoroughly, and then performed an ultrasonication treatment for 10 min to make the ZnS:Cu phosphorescent powder uniformly dispersed into PDMS. By cutting the acrylic plate, 4 cm × 1.5 cm acrylic plate with 1 mm thickness was obtained. The above mixture was then spin-coated onto this acrylic plate. Afterward, it was degassed in a vacuum oven for 10 min. Finally, it was cured and dried in an oven at 80 °C for 2 h.

Fabrication of TENG. A Cu film electrode was attached to the above-mentioned acrylic plate, and then a mixture of PDMS and ZnS:Cu was spin-coated onto the Cu surface. After vacuuming and curing, a PDMS/ZnS:Cu composite with an electrode was fabricated. A circular acrylic plate with a diameter of 1.5 cm was obtained by cutting the acrylic, and a Cu film electrode was pasted. Afterward, the PTFE film was stuck on the Cu surface to obtain the slider with the electrode. The two Cu electrodes were connected to the electrometer for subsequent testing.

Characterization of Materials and the PDMS/ZnS:Cu Composite. The optic fiber would collect the light emission to a spectrometer (NOVA). The electrical signals of the TENG determined by a Keithley 6514 System Electrometer. A microscopic image of the PDMS/ZnS:Cu composite was taken using an environmental scanning electron microscope (ESEM, QUANTA200, Thermo Fisher), whereas the elemental analysis was done by X-ray diffraction (XRD) using a Bruker D8 ADVANCE diffractometer, and the structure of the material was given by a Fourier transform infrared (FTIR, VERTEX80v) spectrophotometer. The X-ray photoelectron spectroscopy (XPS) investigation was measured by an ESCALAB 250Xi spectrometer. The thermodynamic mechanical analysis (TA, Q800) gives the data of the elastic modulus of the PDMS/ZnS:Cu composite at different temperatures.

ASSOCIATED CONTENT

Supporting Information

The Supporting Information is available free of charge at https://pubs.acs.org/doi/10.1021/acsami.1c23155.

XPS and FTIR images of the PDMS; effect of the degree of contact between the triboelectric materials and the PDMS/ZnS:Cu composite on the electric potential; energy of the electron after acceleration under the electric field between the triboelectric materials and the PDMS/ZnS:Cu composite; electric field between the triboelectric materials and the PDMS/ZnS:Cu composite simulated by *Comsol*; potential on the surfaces of the

https://doi.org/10.1021/acsami.1c23155
ACS Appl. Mater. Interfaces 2022, 14, 4775−4782

triboelectric materials and the PDMS/ZnS:Cu composite. (PDF)

AUTHOR INFORMATION

Corresponding Authors

Zhong Lin Wang − *CAS Center for Excellence in Nanoscience, Beijing Key Laboratory of Micro-nano Energy and Sensor, Beijing Institute of Nanoenergy and Nanosystems, Chinese Academy of Sciences, Beijing 101400, P.R. China; School of Nanoscience and Technology, University of Chinese Academy of Sciences, Beijing 100049, P.R. China; CUSTech Institute, Wenzhou, Zhejiang 325024, China; School of Material Science and Engineering, Georgia Institute of Technology, Atlanta, Georgia 30332, United States;* orcid.org/0000-0002-5530-0380; Email: zhong.wang@mse.gatech.edu

Laipan Zhu − *CAS Center for Excellence in Nanoscience, Beijing Key Laboratory of Micro-nano Energy and Sensor, Beijing Institute of Nanoenergy and Nanosystems, Chinese Academy of Sciences, Beijing 101400, P.R. China; School of Nanoscience and Technology, University of Chinese Academy of Sciences, Beijing 100049, P.R. China;* orcid.org/0000-0001-7538-641X; Email: zhulaipan@binn.cas.cn

Authors

Jiayu Li − *CAS Center for Excellence in Nanoscience, Beijing Key Laboratory of Micro-nano Energy and Sensor, Beijing Institute of Nanoenergy and Nanosystems, Chinese Academy of Sciences, Beijing 101400, P.R. China; School of Nanoscience and Technology, University of Chinese Academy of Sciences, Beijing 100049, P.R. China*

Zhiwei Zhang − *CAS Center for Excellence in Nanoscience, Beijing Key Laboratory of Micro-nano Energy and Sensor, Beijing Institute of Nanoenergy and Nanosystems, Chinese Academy of Sciences, Beijing 101400, P.R. China; School of Nanoscience and Technology, University of Chinese Academy of Sciences, Beijing 100049, P.R. China*

Xiongxin Luo − *CAS Center for Excellence in Nanoscience, Beijing Key Laboratory of Micro-nano Energy and Sensor, Beijing Institute of Nanoenergy and Nanosystems, Chinese Academy of Sciences, Beijing 101400, P.R. China; Center on Nanoenergy Research, School of Physical Science & Technology, Guangxi University, Nanning 530004, China*

Complete contact information is available at: https://pubs.acs.org/10.1021/acsami.1c23155

Author Contributions

J.L. and L.Z. conceived the project and designed the experiments. L.Z. and Z.W. guided the project. J.L. performed the experiment and analyzed the data. All the authors discussed and reviewed the manuscript.

Notes

The authors declare no competing financial interest.

ACKNOWLEDGMENTS

This research was supported by the National Natural Science Foundation of China (grants 11704032 and 51432005), the National Key R & D Project from Minister of Science and Technology (2016YFA0202704), and the Beijing Municipal Science & Technology Commission (Z171100000317001, Z171100002017017, and Y3993113DF).

REFERENCES

(1) Becquerel, E. Comptes Rendus Hebdomadaires des Séances de L'Académie des Sciences. *C. R. Acad. Sci.* **1866**, *62*, 999.

(2) Destriau, G. Recherches sur les Scintillations des Sulfures de Zinc Aux Rayons α. *J. Chim. Phys.* **1936**, *33*, 587−625.

(3) Fischer, A. G. Electroluminescent Lines in ZnS Powder Particles. *J. Electrochem. Soc.* **1963**, *110*, 733−748.

(4) Kawashima, S. Blue and Green Luminescence Centers of Electroluminescent ZnS:Cu Phosphors. *Jpn. J. Appl. Phys.* **1966**, *5*, 1161−1170.

(5) Shionoya, S.; Koda, T.; Era, K.; Fujiwara, H. Nature of Luminescence Transitions in ZnS Crystals. *J. Phys. Soc. Jpn.* **1964**, *19*, 1157.

(6) Peka, P.; Schulz, H.-J. Empirical One-Electron Model of Optical Transitions in Cu-doped ZnS and CdS. *Phys. B* **1994**, *193* (1), 57−65.

(7) Bol, A. A.; Ferwerda, J.; Bergwerff, J. A.; Meijerink, A. Luminescence of Nanocrystalline ZnS:Cu^{2+}. *J. Lumin.* **2002**, *99*, 325−334.

(8) Manzoor, K.; Vadera, S. R.; Kumar, N.; Kutty, T. R. N. Multicolor Electroluminescent Devices Using Doped ZnS Nanocrystals. *Appl. Phys. Lett.* **2004**, *84* (2), 284−286.

(9) Wager, J. F.; Keir, P. D. Electrical Characterization of Thin-Film Electroluminescent Devices. *Annu. Rev. Mater. Sci.* **1997**, *27*, 223−248.

(10) Sohn, K.-S.; Timilsina, S.; Singh, S. P.; Choi, T.; Kim, J. S. Mechanically Driven Luminescence in a ZnS:Cu-PDMS Composite. *APL Mater.* **2016**, *4* (10), 106102.

(11) Park, H. J.; Kim, S.; Lee, J. H.; Kim, H. T.; Seung, W.; Son, Y.; Kim, T. Y.; Khan, U.; Park, N. M.; Kim, S. W. Self-Powered Motion-Driven Triboelectric Electroluminescence Textile System. *ACS Appl. Mater. Interfaces.* **2019**, *11* (5), 5200−5207.

(12) Jeong, S. M.; Song, S.; Kim, H.; Joo, K.-I.; Takezoe, H. Mechanoluminescence Color Conversion by Spontaneous Fluorescent-Dye-Diffusion in Elastomeric Zinc Sulfide Composite. *Adv. Funct. Mater.* **2016**, *26* (27), 4848−4858.

(13) Song, S.; Song, B.; Cho, C.-H.; Lim, S. K.; Jeong, S. M. Textile-Fiber-Embedded Multiluminescent Devices: a New Approach to Soft Display Systems. *Mater. Today* **2020**, *32*, 46−58.

(14) Wang, J.; Yan, C.; Chee, K. J.; Lee, P. S. Highly Stretchable and Self-Deformable Alternating Current Electroluminescent Devices. *Adv. Mater.* **2015**, *27* (18), 2876−82.

(15) Stauffer, F.; Tybrandt, K. Bright Stretchable Alternating Current Electroluminescent Displays Based on High Permittivity Composites. *Adv. Mater.* **2016**, *28* (33), 7200−3.

(16) Huang, J.; Yang, Y.; Xue, S.; Yang, B.; Liu, S.; Shen, J. Photoluminescence and Electroluminescence of ZnS:Cu Nanocrystals in Polymeric Networks. *Appl. Phys. Lett.* **1997**, *70* (18), 2335−2337.

(17) Que, W.; Zhou, Y.; Lam, Y. L.; Chan, Y. C.; Kam, C. H.; Liu, B.; Gan, L. M.; Chew, C. H.; Xu, G. Q.; Chua, S. J.; Xu, S. J.; Mendis, F. V. C. Photoluminescence and Electroluminescence from Copper Doped Zinc Sulphide Nanocrystals/Polymer Composite. *Appl. Phys. Lett.* **1998**, *73* (19), 2727−2729.

(18) Peng, W. Q.; Cong, G. W.; Qu, S. C.; Wang, Z. G. Synthesis and Photoluminescence of ZnS:Cu Nanoparticles. *Opt. Mater.* **2006**, *29* (2−3), 313−317.

(19) Wong, M. C.; Chen, L.; Tsang, M. K.; Zhang, Y.; Hao, J. Magnetic-Induced Luminescence from Flexible Composite Laminates by Coupling Magnetic Field to Piezophotonic Effect. *Adv. Mater.* **2015**, *27* (30), 4488−4495.

(20) Jeong, S. M.; Song, S.; Lee, S. K.; Ha, N. Y. Color Manipulation of Mechanoluminescence from Stress-Activated Composite Films. *Adv. Mater.* **2013**, *25* (43), 6194−200.

(21) Wang, Z.-g.; Chen, Y.-f.; Li, P.-j.; Hao, X.; Liu, J.-b.; Huang, R.; Li, Y.-r. Flexible Graphene-Based Electroluminescent Devices. *ACS Nano* **2011**, *5* (9), 7149−7154.

(22) Larson, C.; Peele, B.; Li, S.; Robinson, S.; Totaro, M.; Beccai, L.; Mazzolai, B.; Shepherd, R. Highly Stretchable Electroluminescent Skin for Optical Signaling And Tactile Sensing. *Science* **2016**, *351* (6277), 1071−1074.

(23) Jeong, S. M.; Song, S.; Joo, K.-I.; Kim, J.; Hwang, S.-H.; Jeong, J.; Kim, H. Bright, Wind-Driven White Mechanoluminescence from Zinc Sulphide Microparticles Embedded In A Polydimethylsiloxane Elastomer. *Energy Environ. Sci.* **2014**, *7* (10), 3338−3346.
(24) Shi, X.; Zuo, Y.; Zhai, P.; Shen, J.; Yang, Y.; Gao, Z.; Liao, M.; Wu, J.; Wang, J.; Xu, X.; Tong, Q.; Zhang, B.; Wang, B.; Sun, X.; Zhang, L.; Pei, Q.; Jin, D.; Chen, P.; Peng, H. Large-Area Display Textiles Integrated with Functional Systems. *Nature* **2021**, *591* (7849), 240−245.
(25) Kim, J. S.; Cho, S. H.; Kim, K. L.; Kim, G.; Lee, S. W.; Kim, E. H.; Jeong, B.; Hwang, I.; Han, H.; Shim, W.; Lee, T.-W.; Park, C. Flexible Artificial Synesthesia Electronics with Sound-Synchronized Electroluminescence. *Nano Energy* **2019**, *59*, 773−783.
(26) Cho, S.; Kang, D. H.; Lee, H.; Kim, M. P.; Kang, S.; Shanker, R.; Ko, H. Highly Stretchable Sound-in-Display Electronics Based on Strain-Insensitive Metallic Nanonetworks. *Adv. Sci.* **2021**, *8* (1), 2001647.
(27) Qian, X.; Cai, Z.; Su, M.; Li, F.; Fang, W.; Li, Y.; Zhou, X.; Li, Q.; Feng, X.; Li, W.; Hu, X.; Wang, X.; Pan, C.; Song, Y. Printable Skin-Driven Mechanoluminescence Devices via Nanodoped Matrix Modification. *Adv. Mater.* **2018**, *30* (25), 1800291.
(28) Wang, X.; Zhang, H.; Yu, R.; Dong, L.; Peng, D.; Zhang, A.; Zhang, Y.; Liu, H.; Pan, C.; Wang, Z. L. Dynamic Pressure Mapping of Personalized Handwriting by a Flexible Sensor Matrix Based on the Mechanoluminescence Process. *Adv. Mater.* **2015**, *27* (14), 2324−31.
(29) Zuo, Y.; Xu, X.; Tao, X.; Shi, X.; Zhou, X.; Gao, Z.; Sun, X.; Peng, H. A Novel Information Storage and Visual Expression Device Based on Mechanoluminescence. *J. Mater. Chem. C* **2019**, *7* (14), 4020−4025.
(30) Wei, X. Y.; Wang, X.; Kuang, S. Y.; Su, L.; Li, H. Y.; Wang, Y.; Pan, C.; Wang, Z. L.; Zhu, G. Dynamic Triboelectrification-Induced Electroluminescence and its Use in Visualized Sensing. *Adv. Mater.* **2016**, *28* (31), 6656−64.
(31) Zhao, X. J.; Kuang, S. Y.; Wang, Z. L.; Zhu, G. Electricity-Free Electroluminescence Excited by Droplet Impact Driven Triboelectric Field on Solid-Liquid Interface. *Nano Energy* **2020**, *75*, 104823.
(32) Su, L.; Jiang, Z. Y.; Tian, Z.; Wang, H. L.; Wang, H. J.; Zi, Y. L. Self-powered, ultrasensitive, and high-resolution visualized flexible pressure sensor based on color-tunable triboelectrification-induced electroluminescence. *Nano Energy* **2021**, *79*, 105431.
(33) Su, L.; Wang, H. L.; Tian, Z.; Wang, H. J.; Cheng, Q.; Yu, W. Low Detection Limit and High Sensitivity Wind Speed Sensor Based on Triboelectrification-Induced Electroluminescence. *Adv. Sci.* **2019**, *6*, 1901980.
(34) Lee, B. Y.; Kim, D. H.; Park, J.; Park, K.; Lee, K. J.; Jeong, C. K. Modulation of surface physics and chemistry in triboelectric energy harvesting technologies. *Sci. Technol. Adv. Mater.* **2019**, *20* (1), 758−773.
(35) Wang, Z. L. Triboelectric Nanogenerators as New Energy Technology for Self-Powered Systems and as Active Mechanical and Chemical Sensors. *ACS Nano* **2013**, *7*, 9533−9557.
(36) Zou, H.; Zhang, Y.; Guo, L.; Wang, P.; He, X.; Dai, G.; Zheng, H.; Chen, C.; Wang, A. C.; Xu, C.; Wang, Z. L. Quantifying the Triboelectric Series. *Nat. Commun.* **2019**, *10* (1), 1427.

https://doi.org/10.1021/acsami.1c23155
ACS Appl. Mater. Interfaces 2022, 14, 4775−4782